

LIFT PERFORMANCE OF A TWIST MORPHING MAV WING

N.I. Ismail*, A.H. Zulkifli, M. Hisyam Basri, R.J. Talib and H.Yusoff

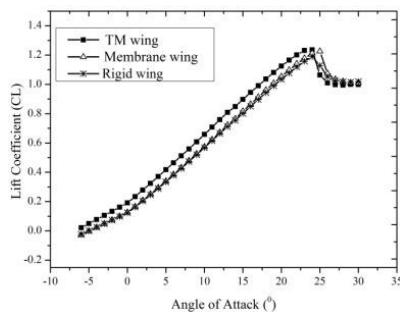
Faculty of Mechanical Engineering, Universiti Teknologi MARA,
13500 Permatang Pauh, Pulau Pinang, Malaysia

Article history

Received
29 January 2015
Received in revised form
28 April 2015
Accepted
09 June 2015

*Corresponding author
iswadi558@ppinang.
uitm.edu.my

Graphical abstract



Abstract

The manoeuvrability performance of a twist morphing MAV has been the main interest for the past researches. However, aerodynamic behaviour of a twist morphing wing is not fully explored due to limited MAV wing size, limited energy budgets, complicated morphing mechanism, and complex aerodynamic-wing structural interaction. Therefore, the effect of a twist morphing wing mobility on the lift distribution of MAV wing is still remained unknown. Thus, present work was carried out to compare the lift performance between a twist morphing wing with membrane and rigid MAV wing design. A quasi-static aeroelastic analysis by using the Ansys-Fluid Structure Interaction (FSI) method is utilized in current works to calculate the lift performance for each MAV wing design. Each MAV wing has identical wing dimension except for twist morphing wing where a 3N morphing force was imposed on the wing to produce the twist mobility. The lift results show that twist morphing wing able to produce (5% to 20%) higher lift magnitude compared to the membrane and rigid wing for every angle attack cases at pre-stall angle. However, twist morphing wing had slightly suffered from (at least 1°) earlier stall angle and produced almost similar maximum lift coefficient magnitude to the membrane wing

Keywords: Micro air vehicle (MAV), fluid structure interaction, morphing wing, aerodynamics

© 2015 Penerbit UTM Press. All rights reserved

1.0 INTRODUCTION

MAV is defined as a small scale aircraft with a wingspan dimension lesser than 15cm, flying at low Reynolds number regime (10^4 – 10^5). MAV is seen to replace unmanned aerial vehicles (UAVs) for futuristic intelligence and surveillance in confined space areas. The rigid wing MAV type is the earliest version of MAV and it can offers better payload and endurance capability[1]. However, this MAV type usually suffers from low lift generation. In order to improve the lift performance, the biological MAV design was used through the application of membrane wing design (passive wing design)[2], [3] and morphing wing design (known as active wing shape adaptation)[4]. Most of these biological

designs are inspired from flying characteristics of airborne mammals, birds[5] and insects[6]. The passive morphing wing (also known as membrane wing design) was developed and showed a significant improvement on the lift generation over MAV wing. However, a successful passive morphing wing had heavily relied on the intensity of wing elasticity. The membrane wing design must undertake a series of aeroelastic tailoring procedure to acquire the right wing stiffness [2], [3]. The application of the active morphing mobility (e.g. twist morphing wing) on an MAV-sized wing is very difficult design task. This is due to the MAV wing size dimension, limited energy, complex morphing mechanism, and high aerodynamic-wing structural interaction[7]–[9]. Thus, earlier research on twist

morphing MAV wing focused more on the manoeuvrability rather than understanding its aerodynamic performance [10], [11]. Consequently, the impact of a twist morphing mobility on lift performances was not fully understood. Thus, present work is carried out to compare the lift performance between a twist morphing wing with membrane and rigid wing design. Here, the lift performance between a twist morphing (TM), membrane and rigid wing are compared to elucidate the lift enhancement produce by a TM MAV wing. A quasi-static aeroelastic analysis by using the Ansys Fluid Structure Interaction (FSI) method is utilized in current works to compare the lift performance between TM, membrane and rigid wing.

2.0 FSI Computation Method

A strong coupled FSI simulation is utilized here to analyze the lift coefficient of twist morphing, membrane and rigid wing. The airflow field is solved using steady state and incompressible turbulent flow boundary conditions. Ansys-CFX module was used in this work and utilized the RANS equations combined with SST $k-\omega$ turbulent model in order to capture the laminar-turbulent transition region. Meanwhile, Ansys-Mechanical module is used to solve the linear-static structural problems on morphing wing. The details of current FSI method is found in reference [12], [13].

3.0 MAV WING MODEL AND BOUNDARY CONDITIONS

3.1 The MAV wing model

In present research, the twist morphing, membrane and rigid MAV wing are modeled based on previous research done at the University of Florida (UF) [2], [3]. The wing model is used due to its natural flexibility characteristics that conducive for morphing mobility. The membrane wing (also known as perimeter reinforce wing) and rigid wing is designated as the baseline model taken from the references [2], [3] with the propeller and stabilizers (horizontal and vertical) are removed for model simplifications. Half wing is implemented for all wing models in order to exploit the symmetrical wing condition. Generally, the present MAV wing designs are almost identical in terms of wing dimension and shape [13]. The wingspan, wing aspect ratio, root chord length and built-in wing twist (and other wing dimension) for each wing is given in Table 1. The distinctive parts among the wings are the morphing force and flexible membrane skin components. All wings configuration are depicted in Figure 1.

The TM wing design is similar to the baseline membrane wing design but with additional morphing force component (3N) imposed at optimized location on the wingtip (90mm from the leading

edge and parallel to wing spanwise axis). The main objective of this morphing force is to produce a twisted wing condition on the morphing wing. The thickness for wing skeleton and membrane skins is maintained at 1.0mm. The origin of the coordinate system is located at the center of the leading edge of the wing and following coordinate system is adopted: x is chordwise, z is spanwise, and y is normal to the wing. The material for wing structure and membrane skin is set to be Perspex [13] and silicone rubber [13], respectively. The detail structural deformation of each wing found in [12] is represented in Figure 2.

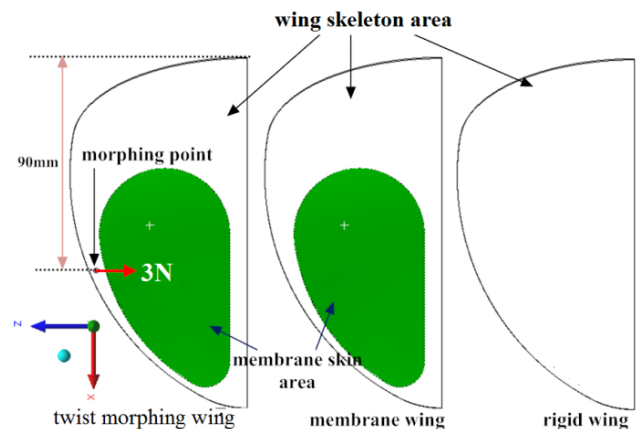


Figure 1 TM (left), membrane (middle) and rigid (right) wing configuration.

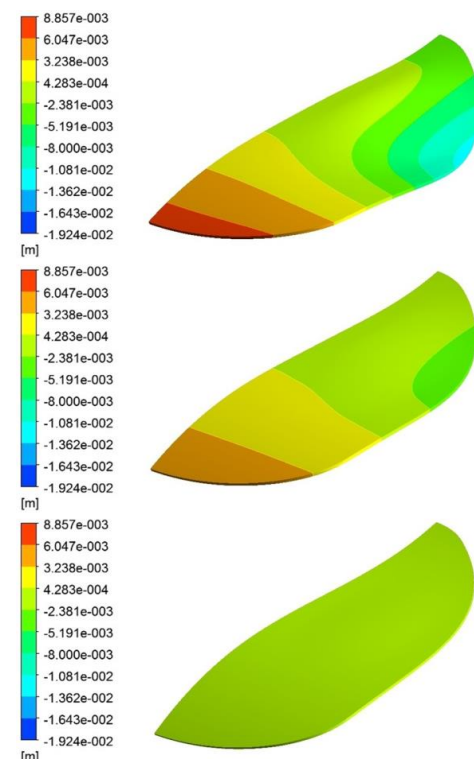


Figure 2 the structural deformation for TM wing (top), membrane (middle) and rigid (bottom) MAV wing.

3.2 Airflow domain

The flow domain (Figure 3) is built surrounding the MAV wing with root chord dimensioned. The flow domain size is

$$17c \text{ (length)} \times 12c \text{ (height)} \times 4c \text{ (wide)}$$

where c is the root chord length of the wing which is approximately 150mm.

The optimized grid is achieved for current flow domain achieved at 1,000,000 elements with $y^+ \leq 1$. The inlet and outlet boundary conditions (Figure 3) applied on the flow domain in which, the inlet velocity magnitude is set at 9.7m/s (equivalent to $Re=100,000$ at chord and the maximum speed for MAV) and zero pressure boundary condition is enforced at the outlet. The angle of attack (AOA) is varied between -7° to 30° with 2° interval. The turbulence intensity of 5% with automatic wall function is also imposed to solve the viscous flow effect over the wings.

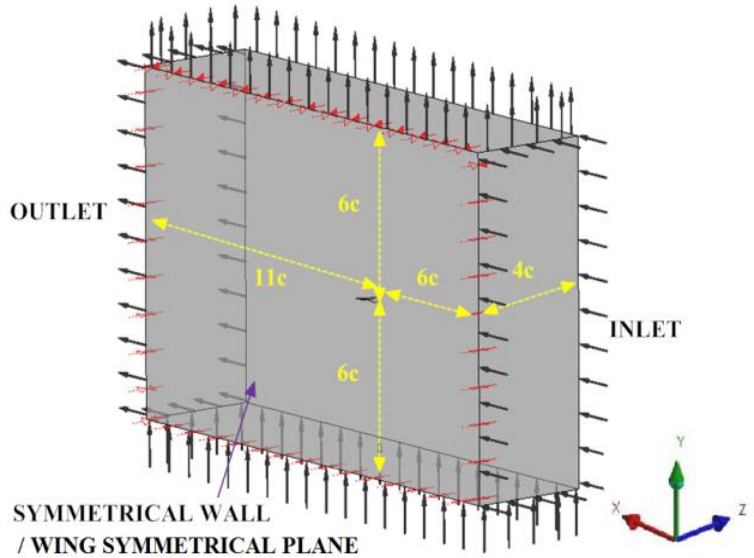


Figure 3 flow domain dimensioned in the wing root chord

Table 1 Wing dimension for TM, membrane and rigid win

	TM Wing	Membrane wing	Rigid wing
Wingspan, b	150mm	150mm	150mm
Root chord, c	150mm	150mm	150mm
Aspect ratio, A	1.25	1.25	1.25
Maximum camber at the root	6.7% of c (at $x/c = 0.3$)	6.7% of c (at $x/c = 0.3$)	6.7% of c (at $x/c = 0.3$)
Maximum reflex at the root	1.4% of c (at $x/c = 0.86$)	1.4% of c (at $x/c = 0.86$)	1.4% of c (at $x/c = 0.86$)
Built-in geometric twist	0.55°	0.55°	0.55°
Force component	Included $F=3N$	Excluded	Excluded
Membrane skin component	Included	Included	Excluded
Approximate membrane skin location	$0.34 \leq x/c \leq 0.9$ $0.10 \leq 2z/b \leq 0.83$	$0.34 \leq x/c \leq 0.9$ $0.10 \leq 2z/b \leq 0.83$	none

4.0 LIFT COEFFICIENT RESULTS

Lift coefficient (C_L) results for all wings are depicted in Figure 4. Generally, the result shows that all wings had exhibited almost similar nonlinear C_L curve towards the angle of attack changes. The non-linear pattern is found for angle of attack (AOA) cases between -7° to 5° . The pattern (non-linear pattern in C_L curve) is commonly found on such low aspect ratio wings due to tip vortex influence as previously shown in reference [14], [15].

Concentrating on the magnitude of C_L , the result shows that TM wing has produced the highest C_L magnitude among the wings. Analytically, the TM wing has an ability to generate approximately 5% to 20% higher C_L magnitude than to the other wings for every angle attack cases below stall angle (AOA stall for TM wing $\approx 24^\circ$) or its pre-stall angle.

TM wing managed to produce approximately 20% higher C_L magnitude (compared to membrane and rigid wing) for AOA cases below 6° . However, the

percentage has decreased when the AOA increased beyond 7° (up to stall angle). TM wing had exhibited only approximately 5% to 15% higher C_L magnitude than other wings at AOA between 7° to 23° . Despite its benevolent performance in C_L magnitude, TM wing has produced similar maximum C_L magnitude (C_{Lmax}) to the membrane wing. Both (TM and membrane) wings managed to produce similar C_{Lmax} at 1.23. However, the aforementioned C_{Lmax} magnitude is approximately 4% higher than the same magnitude produced by rigid wing (C_{Lmax} rigid wing = 1.19). Despite better performance in C_L magnitude, TM wing has slightly suffers from early stall angle (compared to the membrane wing). TM wing is stalled at AOA = 24° , which is 1° earlier than membrane wing. However, TM wing has similar stall angle to the rigid wing.

Based on this result, one can conclude that TM wing able to produce better C_L magnitude than membrane or rigid wing particularly for AOA cases below its stall angle. The enhancement in C_L magnitude for TM wing is contributed by the increment in local AOA magnitude for each wing section as shown in reference [12]. The increment in local AOA magnitude had highly induced a washed-in condition on the TM wing which consequently encourage higher vortex interaction and improved the pressure distribution on the TM wing [12], [13].

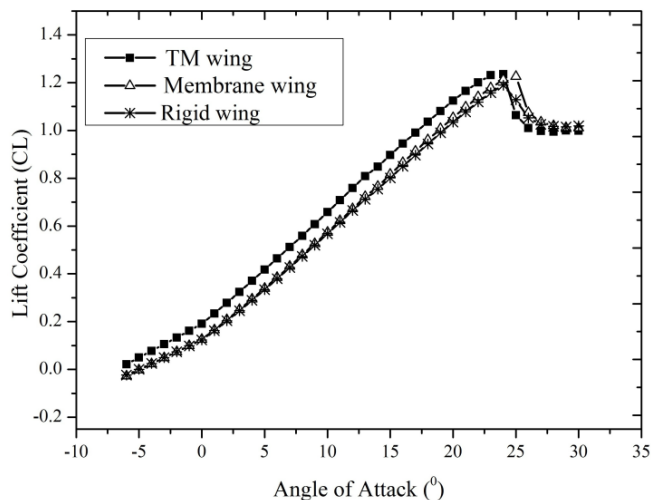


Figure 4 Lift performance for twist morphing, membrane and rigid wings.

5.0 CONCLUSION

Current works is conducted to compare the lift performance between a twist morphing wing with membrane and rigid wing design. Here, two way FSI simulation consists of linear static structural analysis couple with 3D, steady state, incompressible RANS-SST solver was used to solve the wing aerodynamics

problems. The C_L for each wing (twist morphing, membrane and rigid wing) design is presented and compared based on the magnitude of C_L , stall angle and C_{Lmax} . The results exhibited that TM wing able to produce approximately 5% to 20% higher C_L magnitude compared to the other wings for every angle attack cases at pre-stall angle. However, TM wing suffers from earlier stall angle (1° earlier than membrane wing) and produced almost similar C_{Lmax} magnitude to the membrane wing at $C_{Lmax} = 1.23$.

Acknowledgement

The authors acknowledge technical and financial support from Universiti Teknologi MARA and the Government of Malaysia via the sponsorship by the Malaysia Ministry of Higher Education's Fundamental Research Grant Scheme (FRGS) (600-RMI/FRGS 5/3 (152/2014)).

References

- [1] Mohan, S. and Sridharan, G. 2001. Emerging Technologies for Micro-Unmanned Air Vehicles. *Defence Science Journal*. 51(3): 223–228.
- [2] Stanford, B. K. 2008. *Aeroelastic Analysis and Optimization of Membrane Micro Air Vehicle Wings*. Faculty of Graduate School. University Of Florida.
- [3] Stanford, B. K., Ifju, P., Albertani, R. and Shyy, W. 2008. Fixed Membrane Wings For Micro Air Vehicles: Experimental Characterization, Numerical Modeling, And Tailoring. *Progress in Aerospace Sciences*, 44(4): 258–294.
- [4] Abdulrahim, M., Garcia, H. and Lind, R. 2005. Flight Characteristics of Shaping the Membrane Wing of a Micro Air Vehicle. *Journal Of Aircraft*. 42(1): 131–137.
- [5] Supekar, A. H. 2007. *Design, Analysis and Development of A Morphable Wing Structure For Unmanned Aerial Vehicle Performance Augmentation*. Faculty of Graduate School, University of Texas.
- [6] Combes, S. A. and Daniel, T. L. 2003. Flexural stiffness in insect wings II. Spatial distribution and dynamic wing bending. *Journal of Experimental Biology*. 206(17): 2989–2997.
- [7] Chen, Z. 2013. *Micro Air Vehicle Design for Aerodynamic Performance and Flight Stability*. University of Sheffield.
- [8] Banerjee, R. and Seshaiyer, P. 2013. Computational Mechanics of a Coupled Flow-Structure Interaction Problem with Applications to Bio-Inspired Micro Air Vehicles. *International Journal of Aerospace and Lightweight Structures (IJALS)*. 3(3): 399.
- [9] Abudaram, Y. J., Rohde, S., Hubner, J. P. and Ifju, P. 2013. *Composite Materials and Joining Technologies for Composites*. Springer New York.
- [10] Pecora, R., Amoroso, F. and Lecce, L. 2012. Effectiveness of Wing Twist Morphing in Roll Control. *Journal of Aircraft*. 49(6): 1666–1674.
- [11] Vasista, S., Tong, L. and Wong, K. C. 2012. Realization of Morphing Wings: A Multidisciplinary Challenge. *Journal of Aircraft*. 49(1): 11–28.
- [12] Ismail, N. I., Zulkifli, A. H., Abdullah, M. Z., Basri, M. H., Abdullah, N. S., Hisyam Basri, M. and Shah Abdullah, N. 2013. Computational Aerodynamic Analysis on Perimeter Reinforced (PR)-Compliant Wing. *Chinese Journal of Aeronautics*. 26(5): 1093–1105.
- [13] Ismail, N. I., Zulkifli, A. H., Abdullah, M. Z., Basri, M. H. and Abdullah, N. S. 2014. Optimization of aerodynamic

- efficiency for twist morphing MAV wing. *Chinese Journal of Aeronautics*. 27(3): 475–487.
- [14] Colonius, T. and Williams, D. R. 2011. Control of vortex shedding on two- and three-dimensional aerofoils. *Philosophical transactions. Series A, Mathematical, Physical, And Engineering Sciences*. 369(1940): 1525–39.
- [15] Taira, K. and Colonius, T. 2009. Effect of Tip Vortices in Low-Reynolds-Number Poststall Flow Control. *AIAA Journal*. 47(3): 749–756.